

# On the optimum operation conditions of an endoreversible heat engine with different heat transfer laws in the thermal couplings

M.A. Barranco-Jiménez

*Departamento de Ciencias Básicas, Escuela Superior de Cómputo, Instituto Politécnico Nacional,  
Av. Juan de Dios Batiz s/n. Esq. M. Othon de Mendizabal,  
UP Adolfo López Mateos, 07738, México D.F.,  
e-mail: mbarrancoj@ipn.mx*

N. Sánchez-Salas and F. Angulo-Brown

*Departamento de Física, Escuela Superior de Física y Matemáticas, Instituto Politécnico Nacional,  
UP Zacatenco, 07738 México D.F.,  
e-mail: norma@esfm.ipn.mx, angulo@esfm.ipn.mx*

Recibido el 17 de septiembre de 2007; aceptado el 3 de junio de 2008

Within the context of Finite-Time Thermodynamics (FTT) we study the optimum operating conditions of an endoreversible engine model. In this model we consider different heat transfer modes from the hot reservoir to the working fluid, while the mode of heat transfer from the working fluid to the cold reservoir is governed by a Newtonian heat transfer law. In our analysis we use two modes of performance, the maximum power regimen and the so-called ecological function. We calculate the optimum temperatures of the working fluid and the optimum efficiency in terms of the relevant system parameters. We show how the efficiency under a maximum ecological function is greater than the maximum efficiency under maximum power conditions.

*Keywords:* Finite time-thermodynamics; endoreversible engine; optimization.

Dentro del contexto de la Termodinámica de Tiempos Finitos (TTF) se estudian las condiciones de operación óptima de un modelo de máquina térmica endorreversible. En el modelo se consideran diferentes modos de transferencia de calor del almacén caliente a la sustancia de trabajo, mientras que la transferencia de energía de la sustancia de trabajo al almacén frío está dominada principalmente por una ley de enfriamiento tipo Newton. En nuestro estudio consideramos dos regímenes de operación, el de máxima potencia y el de máxima función ecológica. Calculamos las temperaturas óptimas de la sustancia de trabajo, así como la eficiencia óptima de la máquina térmica en función de parámetros representativos del modelo. Se muestra que la eficiencia óptima bajo un régimen de operación ecológica es siempre mayor que la correspondiente eficiencia bajo un régimen de operación de máxima potencia.

*Descriptores:* Termodinámica de tiempos finitos; máquina endorreversible; optimización.

PACS: 44.90.+c

## 1. Introduction

As is well known, the upper bound on the efficiency of a thermal engine operating between two heat reservoirs is the so-called Carnot efficiency, which is given by

$$\eta_C = 1 - \frac{T_L}{T_H}, \quad (1)$$

where  $T_L$  and  $T_H$  are the absolute temperatures of the cold and hot reservoirs, respectively. On the other hand, the efficiency of an endoreversible Carnot engine working under maximum power conditions and considering a Newtonian heat transfer law is given by [1]

$$\eta_{CA} = 1 - \sqrt{\frac{T_L}{T_H}}. \quad (2)$$

The above equation is known in the literature as the Curzon and Ahlborn efficiency and it was also obtained by Chambadal and Novikov at the end of the 50's [2]. In 1991, within the context of FTT an ecological performance criterion for heat engines was proposed by Angulo-Brown [3]. This ecological criterion combines the power output (high

power output) and the entropy generation rate of the power plants (low entropy production) in terms of the maximization of the following expression:

$$E = W - T_L \sigma, \quad (3)$$

where  $W$  is the plant's power output,  $T_L$  is the absolute temperature of the cold reservoir and  $\sigma$  is the total entropy production of the endoreversible power plant model. In general, maximization of the ecological function given by Eq. (3) leads to engine performance with a power output of approximately 75% of the maximum power output and an entropy production of approximately 25% of the entropy produced under maximum power conditions. Furthermore, the ecological criterion has another important property: the efficiency under maximum ecological conditions is approximately the semisum of the efficiencies corresponding to the maximum power regime, given by Eq. (2), and the Carnot efficiency, given by Eq. (1), respectively. Recently Chen *et al.* [4,5] have recognized that the former ecological function is an exergy-based ecological function (for the case  $T_L = T_0$ ,  $T_0$  being the environment temperature). The ecological efficiency [3]

is given by

$$\eta_E \approx \frac{1}{2} (\eta_C + \eta_{CA}) = 1 - \sqrt{\frac{T_L (T_L + T_H)}{2T_H^2}}. \quad (4)$$

Within the context of endoreversible thermal engines, their performance analysis has mainly been done by considering a heat transfer law of cooling of the Newton type. In addition, the use of the same heat transfer law in both thermal couplings (see Fig. 1) with hot and cold reservoirs has been very common [6–9]. However, some authors have considered other heat transfer laws, for instance, a Stefan-Boltzmann law [10–12], or a phenomenological heat transfer law that comes from Irreversible Thermodynamics of the form  $\Delta T^{-1}$  [13, 14] and a Dulong-Petit heat transfer law [15–17], although taking again the same heat transfer law in both hot and cold couplings, respectively. In this work, following Sahin’s procedure [18], we study the optimum operating conditions of an endoreversible engine model. We consider several heat transfer laws from the hot reservoir to the working fluid, while the mode of heat transfer from the working fluid to the cold reservoir is a Newtonian heat transfer law in all the cases considered. In our analysis we use two modes of performance, the maximum power regime and the so-called ecological function. The paper is organized as follows: In Sec. 2, we consider that the heat transfer from the hot reservoir to the working fluid is simultaneously produced by radiation and conduction, while the mode of heat transfer from the working fluid to the cold reservoir is a Newtonian heat transfer law. In this section, we also study the limiting cases when a Newtonian heat transfer law is considered in both the hot and cold reservoirs. In this section, we also consider the case when the heat transfer from the hot reservoir is assumed to be dominated by radiation, while the conduction heat transfer law is assumed to be the main mode of heat transfer to

the low reservoir. In Sec. 3, we analyze the case when the heat transfer from the hot reservoir to the working fluid is given by a heat transfer law of the Dulong-Petit type. Finally, in Sec. 4 we present our conclusions.

## 2. Optimum operation conditions

### 2.1. Heat transfer radiation and heat transfer conduction on the hot side

The endoreversible engine model is shown in Fig. 1. In this model,  $T_a$  and  $T_b$  are the hot and cold sides’ working fluid temperatures, respectively. In this part, we consider that the heat transfer from the hot reservoir to the working fluid is produced by radiation and conduction simultaneously (see Fig. 1), that is,

$$Q_H = C_{HR} (T_H^4 - T_a^4) + C_{HC} (T_H - T_a) \quad (5)$$

where  $C_{HR}$  and  $C_{HC}$  are the thermal conductances in the hot side reservoir. On the other hand, the mode of heat transfer from the working fluid to the cold reservoir is a Newtonian heat transfer law, that is,

$$Q_L = C_{LC} (T_b - T_L), \quad (6)$$

where  $C_{LC}$  is the thermal conductance in the cold side reservoir. According to the first law of thermodynamics, the power output for this heat engine is,

$$W = Q_H - Q_L = \eta_{th} Q_H, \quad (7)$$

where  $\eta_{th} = 1 - (T_b/T_a)$ , and  $W$  and  $Q$ ’s are divided by the cycle’s period. Applying the second law of thermodynamics to the reversible part of the model in Fig. 1, we obtain

$$\frac{Q_H}{T_a} = \frac{Q_L}{T_b}. \quad (8)$$

By using Eqs. (5) and (6) in Eq. (8), a relationship between  $T_a$  and  $T_b$  is obtained as follows,

$$T_b = \frac{T_L}{1 - \frac{C_{HR}}{C_{LC}} \left( \frac{T_H^4 - T_a^4}{T_a} \right) - \frac{C_{HC}}{C_{LC}} \left( \frac{T_H - T_a}{T_a} \right)}. \quad (9)$$

Then, the power output given by Eq. (7) becomes [19]

$$W = [C_{HR} (T_H^4 - T_a^4) + C_{HC} (T_H - T_a)] \left( 1 - \frac{T_b}{T_a} \right) \quad (10)$$

Substituting Eq. (9) into Eq. (10), the non-dimensional power output  $\bar{W} = W/C_{LC}T_H$  can be written as

$$\bar{W} = [r_R (1 - \theta^4) + r_C (1 - \theta)] \times \left[ \frac{(\theta - r_T) - r_R (1 - \theta^4) - r_C (1 - \theta)}{\theta - r_R (1 - \theta^4) - r_C (1 - \theta)} \right], \quad (11)$$

where  $\theta = T_a/T_H$ ,  $r_C = C_{HC}/C_{LC}$ ,  $r_R = C_{HR}T_H^3/C_{LC}$  and  $r_T = T_L/T_H$ . The optimum temperatures  $T_a$  and  $T_b$  under maximum power conditions can be obtained by taking the

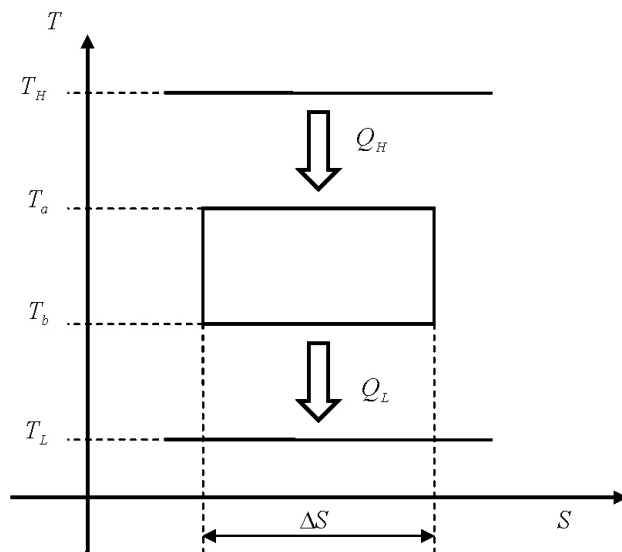


FIGURE 1. Simplified endoreversible solar-driven heat engine model.

derivative of Eq. (11) with respect to  $T_a$ , that is,  $d\bar{W}/d\theta = 0$ . After lengthy algebra the resultant equation to be solved for  $T_a$  is found to be,

$$\begin{aligned}
 0 = & 4r_R^3\theta^{11} + r_R^2(9r_C + 8)\theta^8 - 8r_R^2(r_R + r_C)\theta^7 \\
 & + 2r_R(3r_C^2 + 5r_C + 2)\theta^5 \\
 & - r_R[2(4 + 5r_C)(r_R + r_C) + 3r_T]\theta^4 \\
 & + 4r_R(r_C + r_R)^2\theta^3 + r_C(1 + r_C)^2\theta^2 \\
 & - 2(r_C + r_C^2)(r_C + r_R)\theta + (r_C + r_R) \\
 & \times [r_C(r_C + r_R) - r_T]. \tag{12}
 \end{aligned}$$

The solution to Eq. (12) can be found numerically. It should be noted that the physically meaningful root of  $\theta$  in Eq. (12) is that which is located between 0 and 1. When the heat transfer by radiator is not considered in the hot side, that is,  $r_R \rightarrow 0$ , Sahin [18] showed that the optimum operation condition is given by

$$\theta \rightarrow \frac{r_C + \sqrt{r_T}}{1 + r_C}, \tag{13}$$

this equation indicates that as  $r_T$  (i.e.  $T_L$ ) increases  $\theta$  increases, that is, the optimum value of  $T_a$  for a fixed value of  $T_H$ . Since  $T_a/T_L = \theta/r_T$  and using Eq. (13), Sahin [18] also showed that,

$$\frac{T_a}{T_L} = \frac{r_C + \sqrt{r_T}}{r_T(1 + r_C)} \tag{14}$$

and

$$\frac{T_b}{T_L} = \frac{r_C + \sqrt{r_T}}{\sqrt{r_T}(1 + r_C)}; \tag{15}$$

thus the efficiency for this case approaches the Curzon-Alborn efficiency given by Eq. (1), that is,

$$\eta_{CA} = 1 - \sqrt{r_T}.$$

To investigate the optimum operation conditions under the maximum ecological function, we calculate the total entropy production. Applying the second law of thermodynamic to the model of Fig. 1, the total entropy production  $\sigma$  can be expressed as

$$\sigma = \frac{Q_L}{T_L} - \frac{Q_H}{T_H} \tag{16}$$

Using Eqs. (3), (11) and (16), the non-dimensional ecological function  $\bar{E} = E/C_{LC}T_H$  can be expressed as,

$$\begin{aligned}
 \bar{E} = & [r_R(1 - \theta^4) + r_C(1 - \theta)] \\
 & \times \left[ 1 + r_T - \frac{2r_T}{\theta - r_R(1 - \theta^4) - r_C(1 - \theta)} \right]. \tag{17}
 \end{aligned}$$

In the previous equation we used Eqs. (5) and (6). Analogously to the maximum power conditions, the optimum temperatures  $T_a$  and  $T_b$  under maximum ecological conditions

is obtained by differentiating (17) with respect to  $T_a$ , that is,  $d\bar{E}/d\theta = 0$ , and the resultant equation to be solved for  $T_a$  is found to be

$$\begin{aligned}
 0 = & 4r_R^3\theta^{11} + r_R^2(9r_C + 8)\theta^8 - 8r_R^2(r_R + r_C)\theta^7 \\
 & + 2r_R(3r_C^2 + 5r_C + 2)\theta^5 \\
 & - r_R \left[ 2(4 + 5r_C)(r_R + r_C) + \frac{6r_T}{1 + r_T} \right] \theta^4 \\
 & + 4r_R(r_C + r_R)^2\theta^3 + r_C(1 + r_C)^2\theta^2 \\
 & - 2r_C(1 + r_C)(r_C + r_R)\theta \\
 & + (r_C + r_R) \left[ r_C(r_C + r_R) - \frac{2r_T}{1 + r_T} \right]. \tag{18}
 \end{aligned}$$

Analogously to the maximum power conditions, the solution to Eq. (18) is obtained numerically, and the physically meaningful root of  $\theta$  in Eq. (18) is also located between 0 and 1. However, when  $r_R \rightarrow 0$ , the optimum operation conditions are now given by

$$\lim_{r_R \rightarrow 0} \theta = \frac{r_C(1 + r_T) + \sqrt{2r_T(1 + r_T)}}{(1 + r_C)(1 + r_T)} \tag{19}$$

Therefore, by using Eq. (9) we can obtain that efficiency for this case approaches the ecological efficiency given by Eq. (4), that is

$$\lim_{r_R \rightarrow 0} \eta \rightarrow \eta_E = 1 - \sqrt{\frac{r_T(1 + r_T)}{2}}.$$

### 2.1.1. Numerical calculations

For a numerical calculation, the temperature of a typical low temperature reservoir is taken as  $T_L=300\text{K}$ . Then, the efficiency under maximum ecological conditions and optimum values of the temperatures  $T_a$  and  $T_b$  can be studied. We compared our obtained results with those obtained by Sahin [18] under maximum power conditions. In Fig. 2a, we show the variation of  $\theta$  with respect to  $r_R$  for three different values of  $r_T$  and  $r_C = 0.1$ . We can see as the radiation term ( $r_R$ ) increases,  $\theta$  increases and approaches 1, under both the maximum power and maximum ecological conditions. This means that the optimal temperature  $T_a$  gets closer to the source temperature  $T_H$  as radiation increases. For higher values of  $r_T$ , the ratio of the optimum temperature  $T_a$  to the source temperature  $T_H$  is higher in general. In Fig. 2b, we show the effect of the convection ( $r_C$ ) on the optimum temperature variation  $\theta$  for a fixed value of  $r_R = 0.1$  and for three different values of  $r_T$ . We can see how  $\theta$  reaches a weak minimum and then increases as  $r_C$  increases, and higher values of  $r_T$  yields higher values of  $\theta$ . In Figs. 3a and 3b, we show the variation of optimum temperatures  $T_a$  and  $T_b$  versus  $r_R$  (with  $r_C = 0.1$ ) and  $r_C$  (with  $r_R = 0.1$ ), respectively. As we can see, in Fig. 3a while  $r_R$  tends to 1, the difference between  $T_a$  and  $T_L$  increases. However,  $T_b$  approaches

a constant value as  $r_R$  increases. In Fig. 3b, the optimum temperature variations with respect to  $r_C$  are given for fixed values of  $r_R = 0.1$  and  $r_T = 0.1$ . As we can see,  $T_b/T_L$  increases while  $T_a/T_L$  initially decreases to a minimum and then increases as  $r_C$  increases and the gap between  $T_a$  and  $T_b$  also increases. In Fig. 4a, we show the variation of the efficiencies under maximum power and maximum ecological conditions versus  $r_R$  for three different values of  $r_C$  and for a fixed value of  $r_T = 0.1$ . As we can observe, for all the interval of values of  $r_R$  the efficiency under maximum ecological conditions is greater than the efficiency under maximum power conditions. The difference in the efficiencies is greater for smaller  $r_C$  values and as  $r_R$  increases, the efficiencies reach a maximum and then decrease. In Fig. 4b, the effect the convection on the efficiencies is given for a fixed value of  $r_T = 0.1$  and for three different values of  $r_R$ . Analogously to figure 4a, in this case for the entire interval of values of  $r_C$ , the efficiency under maximum ecological conditions is greater than the efficiency under maximum power conditions.

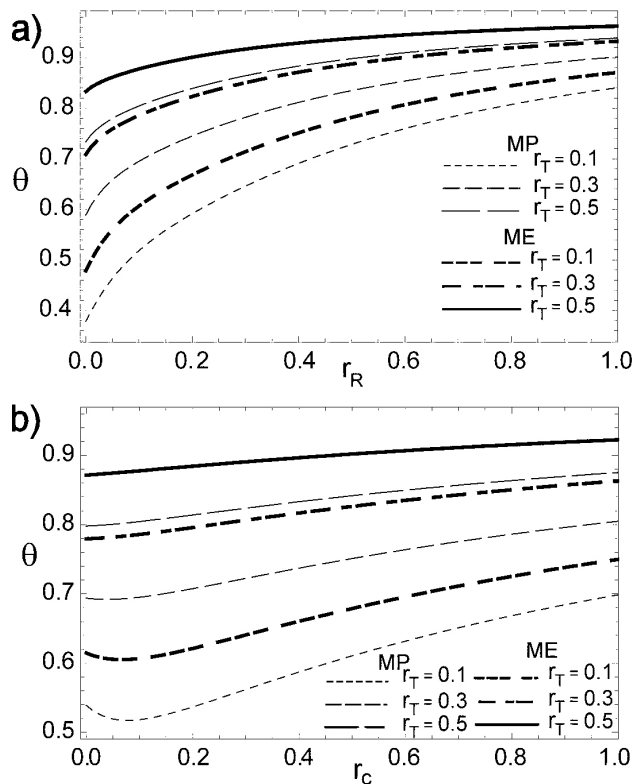


FIGURE 2. a) Numerical roots  $\theta$  of Eqs. (12) and (18), at maximum power and maximum ecological function, respectively, vs.  $r_R$ , with  $r_C = 0.1$ . b) Numerical roots  $\theta$  of Eqs. (12) and (18), at maximum power and maximum ecological function, respectively, vs.  $r_C$ , with  $r_R = 0.1$ . In both cases for several values of  $r_T$ .

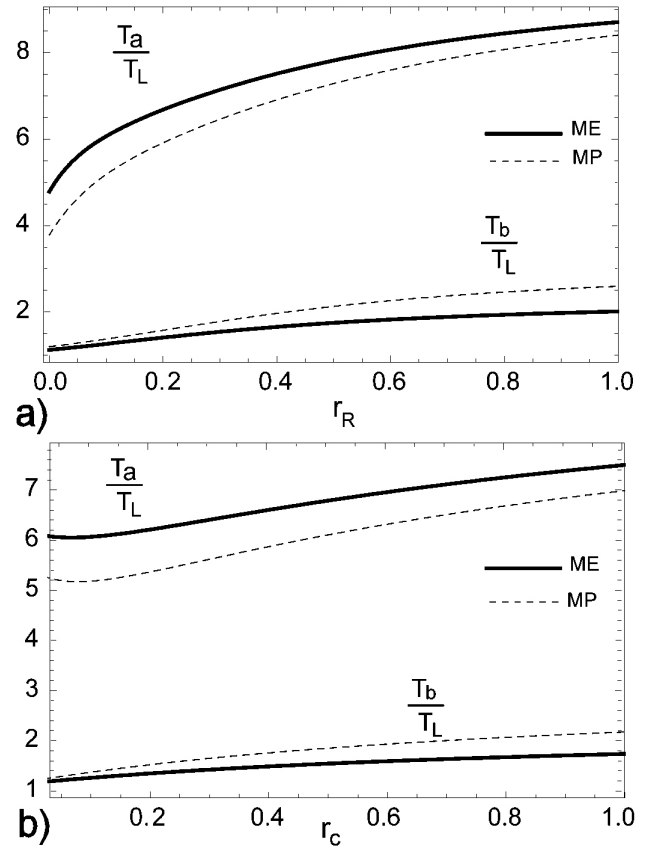


FIGURE 3. a) Optimal temperatures  $T_b$  and  $T_a$  vs.  $r_R$  for  $r_C=0.1$ . b) Optimal temperatures  $T_b$  and  $T_a$  vs.  $r_C$  for  $r_R = 0.1$ . In both cases  $r_T = 0.1$ .

### 2.2. Heat transfer by radiation on the hot side

We now consider that the heat transfer from the hot reservoir to the working fluid is given only by radiation while the heat transfer from the working fluid to the cold reservoir is a Newtonian heat transfer law (see Fig. 1), which can be expressed as

$$Q_H = C_H (T_H^4 - T_a^4) \tag{20}$$

$$Q_L = C_L (T_b - T_L), \tag{21}$$

respectively, where  $C_H$  and  $C_L$  are the thermal conductances for the hot and cold side reservoirs respectively. Substituting Eqs. (20) and (21) into Eq. (8), the relationship between  $T_a$  and  $T_b$  is now given by

$$T_b = \frac{T_L}{1 - \frac{C_H}{C_L} \left( \frac{T_H^4 - T_a^4}{T_a} \right)} \tag{22}$$

Then, the non-dimensional power output  $\bar{W} = W/C_L T_H$  can now be written as

$$\bar{W} = r_C (1 - \theta^4) \left[ \frac{\theta - r_C (1 - \theta^4) - r_T}{\theta - r_C (1 - \theta^4)} \right], \tag{23}$$

where  $\theta = T_a/T_H$ ,  $r_C = C_H T_H^3 / C_L$  and  $r_T = T_L/T_H$ . Analogously to the previous subsection, the optimum tem-

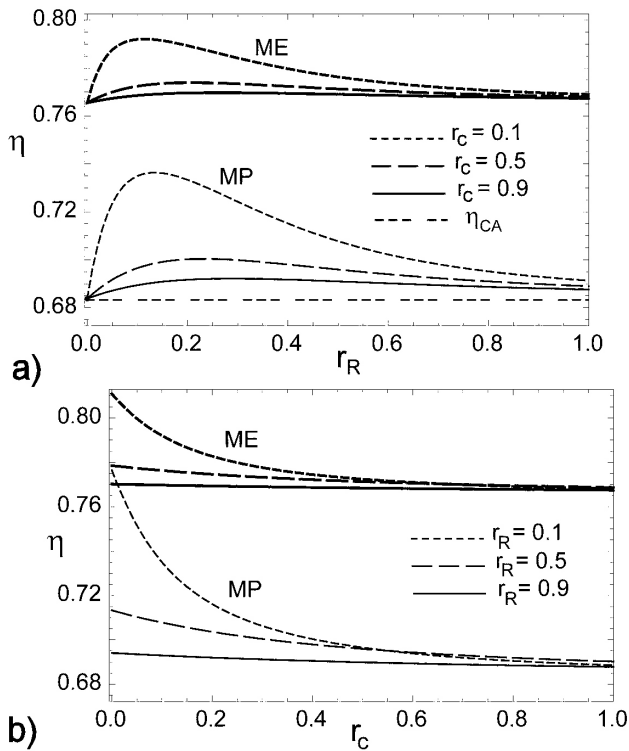


FIGURE 4. a) Optimal efficiency  $\eta$  vs.  $r_R$ , with  $r_T = 0.1$  for  $r_C = 0.1$ ,  $r_C = 0.5$  and  $r_C = 0.9$ , respectively. b) Optimal efficiency  $\eta$  vs.  $r_C$ , with  $r_T = 0.1$ , for  $r_R = 0.1$ ,  $r_R = 0.5$  and  $r_R = 0.9$ , respectively.

peratures  $T_a$  and  $T_b$  under maximum power conditions can be also obtained by differentiating Eq. (23) with respect to  $T_a$ , that is,

$$\begin{aligned} \frac{d\bar{W}}{d\theta} &= 4r_C^2\theta^{11} + 8r_C\theta^8 - 8r_C^2\theta^7 \\ &+ 4\theta^5 - (8r_C + 3r_T)\theta^4 \\ &+ 4r_C^2\theta^3 - r_T = 0. \end{aligned} \tag{24}$$

On the other hand, by using Eqs. (16) and (23) in the ecological function given by Eq. (3), we obtain the non dimensional ecological function  $\bar{E} = E/C_L T_H$  as

$$\begin{aligned} \bar{E} &= r_C (1 - \theta^4) \\ &\times \left[ \frac{(1 + r_T)\theta - r_C(1 + r_T)(1 - \theta^4) - 2r_T}{\theta - r_C(1 - \theta^4)} \right]; \end{aligned} \tag{25}$$

in this case, the optimum temperatures  $T_a$  and  $T_b$  under maximum ecological conditions are also obtained by

$$\begin{aligned} \frac{d\bar{E}}{d\theta} &= 2r_C^2(1 + r_T)\theta^{11} + 4r_C(1 + r_T)\theta^8 \\ &- 4r_C^2(1 + r_T)\theta^7 + 2(1 + r_T)\theta^5 \\ &- (4r_C + 3r_T + 4r_C r_T)\theta^4 \\ &+ 2r_C^2(1 + r_T)\theta^3 - r_T = 0. \end{aligned} \tag{26}$$

In the same way as in the previous section, the solution to Eqs. (24) and (26) is obtained numerically, and the physically meaningful roots of  $\theta$  are also located between 0 and 1.

2.2.1. Numerical calculations

For the numerical calculation, the temperature of a typical low temperature reservoir is taken as  $T_L=300\text{K}$ , and we compared our results obtained under maximum ecological conditions with those obtained by Sahin [18] under maximum power conditions. In this section, our analysis is done in two cases by fixing one of the parameters  $r_T$  and  $r_C$  in each case and studying the effect of the other on the efficiencies and the optimum temperatures. In Fig. 5, the roots of Eqs. (24) and (26) are shown as a function of the parameter  $r_C$  by using three different values of  $r_T$ . We observe that under maximum power conditions as  $r_C$  is increased from 0 to  $\infty$ ,  $\theta$  varies between 0.494 and 1 for  $r_T = 0.1$ ; between 0.649 and 1 for  $r_T = 0.3$  and between 0.757 and 1 for  $r_T = 0.5$  respectively. In the case of maximum ecological conditions we can observe that as  $r_C$  increases from 0 to  $\infty$ ,  $\theta$  varies between 0.576 and 1 for  $r_T = 0.1$ ; between 0.749 and 1 for  $r_T = 0.3$ ; and between 0.841 and 1 for  $r_T = 0.5$ , respectively. In Fig. 6, we show the variation of the efficiencies versus  $r_C$  for a fixed value of  $r_T = 0.3$ . In this figure, the Carnot (0.7) and Curzon and Ahlborn (0.452) efficiencies are also included for comparison. As we can see in Fig. 6, for the entire interval of values of  $r_C$  the efficiency under maximum ecological conditions is bigger than the efficiency under maximum power conditions. The optimum temperature variations with respect to  $r_C$  are shown in Fig. 7. The optimum values of  $T_a$  and  $T_b$  increase as  $r_C$  increases. As we can see under maximum power conditions, as  $r_C$  varies from 0 to  $\infty$ ,  $T_a$  increases from 649 to 1000K, and  $T_b$  increases from 300 to 547K, while under maximum ecological conditions, as  $r_C$  varies from 0 to  $\infty$ ,  $T_a$  increases from 742.4 to 1000K, and  $T_b$  increases from 300 to 547K. On the other hand, to study the effect of  $r_R$  on both the efficiencies and the optimum temperature values, the value of  $r_C$  is now fixed. In Figs. 8 we show the variation of  $\theta$  with respect to  $r_T$  for different values of  $r_C$  under both the maximum power and ecological conditions. As we can see under both the maximum power and ecological conditions,  $\theta$  sharply increases and reaches 1 as  $r_T$  approaches 1. However, under maximum power conditions at  $r_T = 0$ ,  $\theta$  takes on values of 0.237, 0.738 and 0.976 for the fixed values of  $r_C$  equal to 0.1, 1 and 10, respectively, while under maximum ecological conditions,  $\theta$  takes on values of 0.237, 0.738 and 0.976 for the fixed values of  $r_C$  equal to 0.1, 1 and 10, respectively. The variation of the efficiencies with respect to  $r_T$  is shown in Fig. 9. Analogously to the previous case, in this situation, for the entire interval of values of  $r_T$  the efficiency under maximum ecological conditions is greater than the efficiency under maximum power conditions. The differences between the efficiencies is greater for small values of  $r_T$ . Which is expected for typical heat engines. Finally, the variation of the optimum temperatures with respect

to  $r_T$  is given in Fig. 10. We can observe, under both the maximum power and the ecological conditions, a considerable gap that is to be expected between  $T_a$  and  $T_b$  for small values of  $r_T$ . However, this difference decreases to zero as  $r_T$  approaches 1.

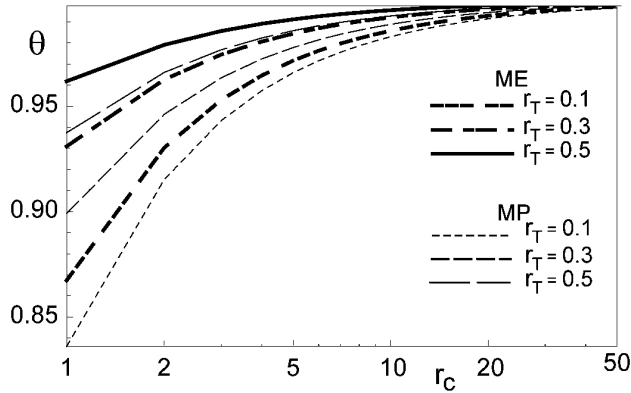


FIGURE 5. Numerical roots of Eq.(24), maximum power, and Eq.(26), maximum ecological function, vs.  $r_C$ , with  $r_T = 0.1$ ,  $r_T = 0.3$  and  $r_T = 0.5$ .

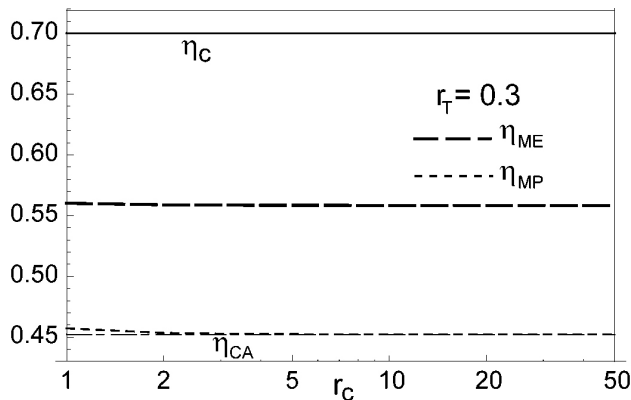


FIGURE 6. Optimal efficiencies (maximum power and maximum ecological function) vs.  $r_C$ , with  $r_T = 0.3$ . Also  $\eta_C$  and  $\eta_{CA}$  are plotted.

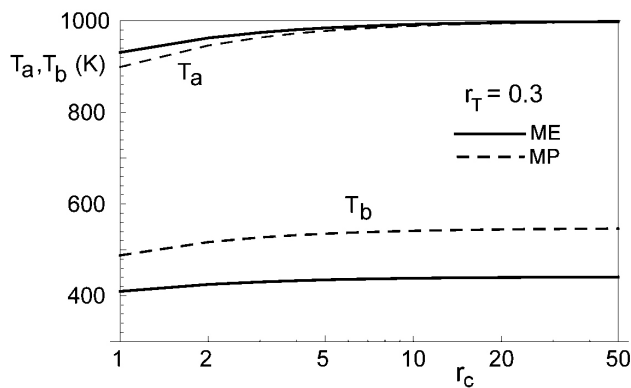


FIGURE 7. Optimal temperatures  $T_b$  and  $T_a$ , vs.  $r_C$  with  $r_T = 0.3$ .

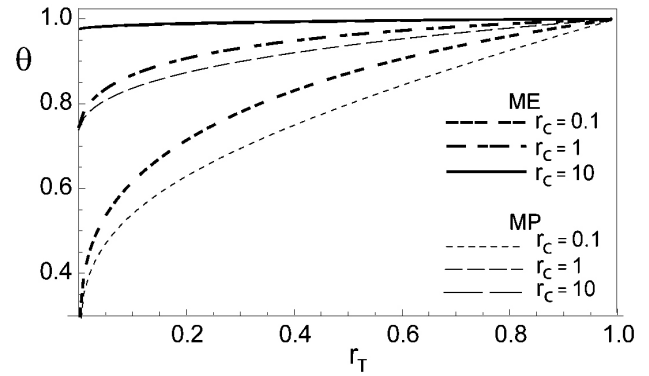


FIGURE 8. Numerical roots  $\theta$  of Eq. (24), maximum power and Eq. (26) maximum ecological function, vs.  $r_T$ , with  $r_C = 0.1$ ,  $r_C = 1$  and  $r_C = 10$ .

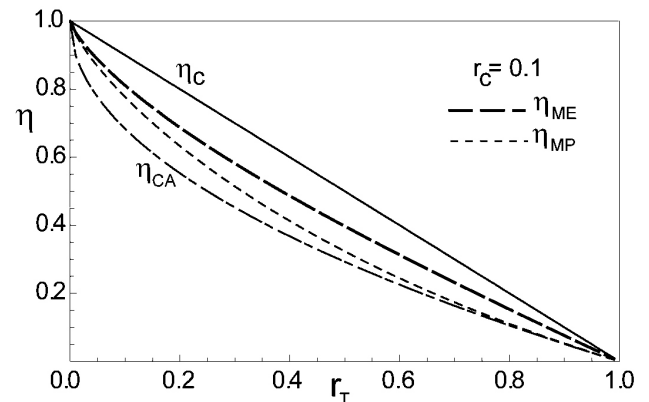


FIGURE 9. Optimal efficiencies vs.  $r_T$  with  $r_C = 0.1$ . Also  $\eta_C$  and  $\eta_{CA}$  are plotted.

### 3. Optimum operation conditions with heat transfer of the Dulong-Petit type on the hot side

It has been recognized in the literature [20] that a more realistic description of the heat exchange between the working substance and its reservoirs would include a  $T^4$  term (Stefan-Boltzmann radiation). An attempt to describe combined conductive-convective and radiative cooling by a power-law relationship is given by the so-called Dulong-Petit law of cooling [20], which is

$$\frac{dQ}{dt} = \alpha (T_a - T)^n, \tag{27}$$

where  $dQ/dt$  is the rate of heat loss per unit area from a body at temperature  $T$ ,  $\alpha$  is a thermal conductance,  $T_a$  is the temperature of the fluid surrounding the body, and  $n$  is an exponent with a value between 1.1 and 1.6 [20]. Some authors have established that  $n = 5/4$  based on studies made by Lorentz and Langmuir. As O'Sullivan asserts in his original 1879 paper, Stefan took the results of Dulong and Petit (DP), along with experiments by Tyndall, and pointed out that the DP model was in agreement with his  $T^4$  law [20]. In the present paper we use the DP law of cooling with  $n = 5/4$ .

Now, we consider that the heat transfer from the hot reservoir to the working fluid is given by a heat transfer law of the Dulong-Petit type, while the heat transfer from the cold reservoir is a Newtonian heat transfer law in the same way as in the previous section (see Fig. 1), which can be expressed as

$$Q_H = C_H (T_H - T_a)^{\frac{5}{4}} \quad (28)$$

Substituting Eqs. (6) and (28) into Eq. (8), the relationship between  $T_a$  and  $T_b$  is now given by

$$T_b = \frac{T_L}{1 - \frac{C_H}{C_L} \left( \frac{(T_H - T_a)^{\frac{5}{4}}}{T_a} \right)} \quad (29)$$

Using Eqs. (6), (7), (28) and (29), the non-dimensional power output  $\bar{W} = W/C_L T_H$  can now be written now as

$$\bar{W} = r_C (1 - \theta)^{\frac{5}{4}} \left[ \frac{\theta - r_C (1 - \theta)^{\frac{5}{4}} - r_T}{\theta - r_C (1 - \theta)^{\frac{5}{4}}} \right], \quad (30)$$

where  $\theta = T_a/T_H$ ,  $r_C = C_H T_H^{\frac{1}{4}}/C_L$  and  $r_T = T_L/T_H$ . Analogously to the previous section, the optimum temperatures  $T_a$  and  $T_b$  under maximum power conditions can also be obtained by taking the derivative of Eq. (30) with respect to  $T_a$ , that is,

$$r_T (4 + \theta) - 5 \left( \theta - r_C (1 - \theta)^{\frac{5}{4}} \right)^2 = 0 \quad (31)$$

On the other hand, using Eqs. (16) and (30) in the ecological function given by Eq. (3), we obtain the non-dimensional ecological function as

$$\bar{E} = r_C (1 - \theta)^{\frac{5}{4}} \times \left[ \frac{(1 + r_T) \theta - r_C (1 + r_T) (1 - \theta)^{\frac{5}{4}} - 2r_T}{\theta - r_C (1 - \theta)^{\frac{5}{4}}} \right]; \quad (32)$$

in this case, the optimum temperatures  $T_a$  and  $T_b$  under maximum ecological conditions are also obtained by

$$5 \left( \theta - r_C (1 - \theta)^{\frac{5}{4}} \right)^2 + r_T \left( 5 \left( \theta - r_C (1 - \theta)^{\frac{5}{4}} \right)^2 - 2(4 + \theta) \right) = 0. \quad (33)$$

In the same way as in the previous section, the solution of Eqs. (31) and (33) is found numerically, and the physically meaningful roots of  $\theta$  are also located between 0 and 1.

### 3.0.2. Numerical calculations

In a similar way to Sec. 2.2.1, for a numerical calculation, the temperature of a typical low temperature reservoir is taken as  $T_L = 300K$ . In this section, our analysis is done in two cases by fixing one of the two parameters  $r_T$  and  $r_C$  in each case and studying the effect of the other on the efficiencies

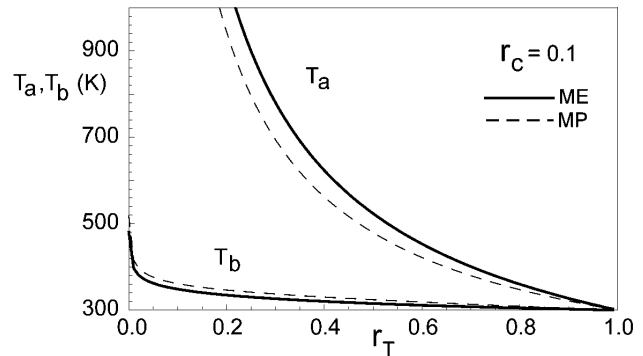


FIGURE 10. Optimal temperatures  $T_a$  and  $T_b$  vs.  $r_T$  with  $r_C=0.1$ .

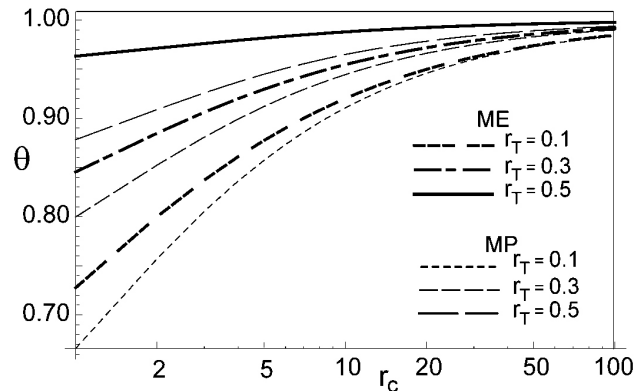


FIGURE 11. Numerical roots  $\theta$  of Eq.(31), maximum power and Eq.(33), maximum ecological function, vs.  $r_C$ , with  $r_T = 0.1$ ,  $r_T = 0.3$  and  $r_T = 0.5$ .

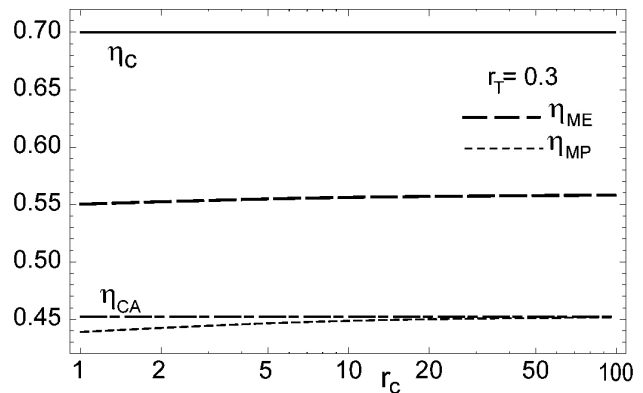


FIGURE 12. Optimal efficiencies (maximum power and maximum ecological function) vs.  $r_C$ , with  $r_T = 0.3$ .

and the optimum temperatures. In Fig. 11, the roots of Eqs. (31) and (33) are shown as a function of the parameter  $r_C$  by using three different values of  $r_T$ . We observe that under maximum power conditions as  $r_C$  is increased from 0 to  $\infty$ ,  $\theta$  varies between 0.299 and 1 for  $r_T = 0.1$ , 0.525 and 1, respectively, for  $r_T = 0.3$ , and between 0.685 and 1 for  $r_T = 0.5$ . In the case of maximum ecological conditions we can observe that as  $r_C$  increases from 0 to  $\infty$ ,  $\theta$  varies between 0.405 and 1 for  $r_T = 0.1$ ; between 0.658 and 1 for  $r_T = 0.3$ ; and between 0.801 and 1 for  $r_T = 0.5$ , respectively. In Fig. 12, we show the variation of the efficiencies

versus  $r_C$  for a fixed value of  $r_T = 0.3$ . In this figure, the values of both the Carnot (0.7) and Curzon and Ahlborn (0.452) efficiencies are also included for comparison. As we can see in Fig. 12, for all the interval of values of  $r_C$  the efficiencies satisfy the relation  $\eta_{MP} < \eta_{CA} < \eta_E < \eta_C$ , when  $r_C = 0$ ,  $\eta_{MP} = 0.423$  and  $\eta_E = 0.542$ . The optimum temperature variations with respect to  $r_C$  are shown in Fig. 13. The optimum values of  $T_a$  and  $T_b$  increase as  $r_C$  increases. As we can see under maximum power conditions, as  $r_C$  varies from 0 to  $\infty$ ,  $T_a$  increases from 520 to 729K, and  $T_b$  increases from 300 to 410K, while under maximum ecological conditions, as  $r_C$  varies from 0 to  $\infty$ ,  $T_a$  increases from 655 to 800K, and  $T_b$  increases from 300 to 360K. On the other hand, to study the effect of  $r_R$  on both the efficiencies and the optimum temperature values, the value of  $r_C$  is now fixed. In Fig. 14 we show the variation of  $\theta$  with respect to  $r_T$  for different values of  $r_C$ . As we can observe for both the maximum power and ecological conditions,  $\theta$  sharply increases and reaches 1 as  $r_T$  approaches 1. However, under maximum power conditions at  $r_T = 0$ ,  $\theta$  takes on values of 0.237, 0.738 and 0.976 for the fixed values of  $r_C$  equal to 0.1, 1 and 10, respectively, while under maximum ecological conditions,  $\theta$  takes on values of 0.237, 0.738 and 0.976 for the fixed values of  $r_C$  equal to 0.1, 1 and 10, respectively.

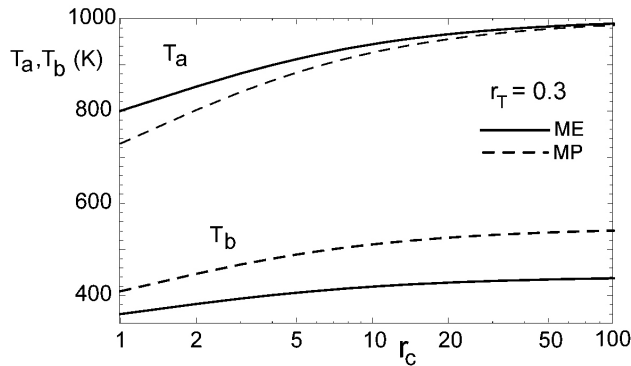


FIGURE 13. Optimal temperatures  $T_b$  and  $T_a$ , vs.  $r_C$  with  $r_T = 0.3$ .

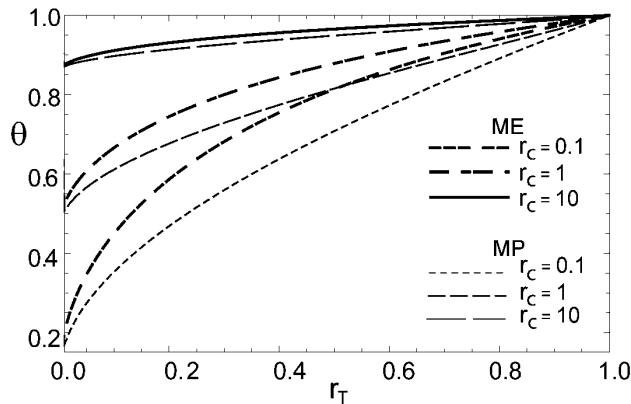


FIGURE 14. a) Numerical roots  $\theta$  of Eq. (31), maximum power and Eq. (33) b) maximum ecological function, vs.  $r_T$ , with  $r_C = 0.1$ ,  $r_C = 1$  and  $r_C = 10$ .

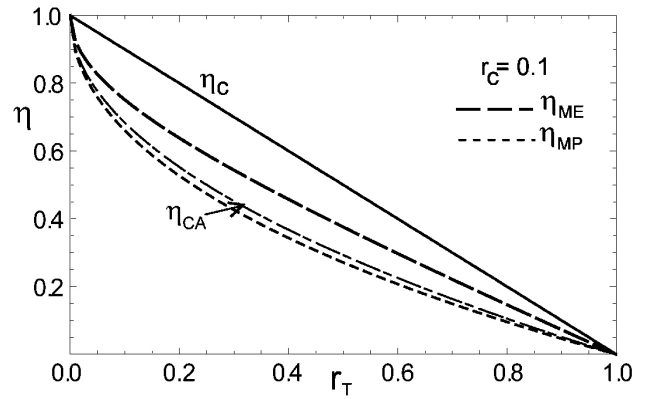


FIGURE 15. Optimal efficiencies vs.  $r_T$  with  $r_C = 0.1$ .

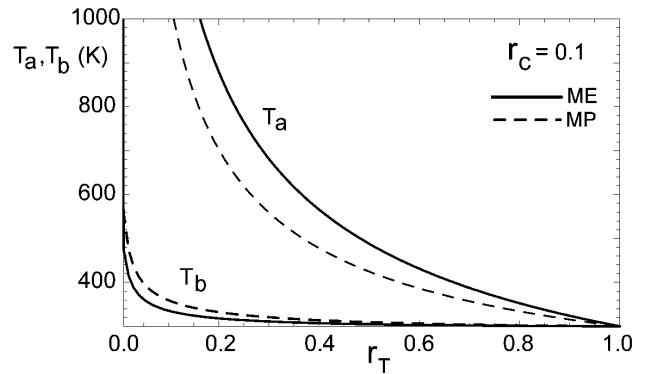


FIGURE 16. Optimal temperatures  $T_a$  and  $T_b$  vs.  $r_T$  with  $r_C = 0.1$ .

The variation of the efficiencies with respect to  $r_T$  is shown in Fig. 15; in this case, for the entire interval of values of  $r_T$  the efficiency under maximum ecological conditions is greater than the efficiency under maximum power conditions and it also satisfies the relation  $\eta_{MP} < \eta_{CA} < \eta_E < \eta_C$ . Finally, the variation of the optimum temperatures with respect to  $r_T$  is given in Fig. 16. We can observe, for both the maximum power and the ecological conditions, a considerable gap that is to be expected between  $T_a$  and  $T_b$  for small values of  $r_T$ . However, this difference decreases to zero as  $r_T$  approaches 1.

#### 4. Conclusions

Within the context of Finite-Time Thermodynamics we analyzed the optimum operating conditions of an endoreversible engine model. Practically all of the thermal engine FTT-models published until now [21–24] have considered the same heat transfer law at both couplings between the reservoirs and the working fluid. In the model presented here, we considered different heat transfer laws from the hot reservoir to the working fluid, while the mode of heat transfer from the working fluid to the cold reservoir is a Newtonian linear law in all cases. We calculated the optimum temperatures of the working fluid and the optimum efficiency in terms of the relevant system parameters by considering two modes of performance, the maximum power regime and the so-called

ecological function. We show how the efficiency under maximum ecological function is greater than the maximum efficiency under maximum power conditions. This result has systematically been observed in all kinds of thermal engine models operating under ecological conditions. This property is considered to be concomitant with ecological goals from a long-term energy conversion point of view.

## Acknowledgments

This work was supported in part by COFAA and EDI-IPN-México.

- 
1. F. Curzon and B. Ahlborn, *Am. J. Phys.* **43** (1975) 22.
  2. P. Chambadal, *Rev. Gén. Électr.* **67** (1958) 332; Novikov II. *J. Nuclear Energy.* **7** (1958) 125.
  3. F. Angulo-Brown, *J. Appl. Phys.* **69** (1991) 7465.
  4. J. Chen *et al.*, *Applied Energy.* **83** (2006) 573.
  5. X. Zhu *et al.*, *J. of the Energy Institute* **7** (2006) 42.
  6. P. Salamon and A. Nitzan, *J. Chem. Phys.* **74** (1986) 3546.
  7. A. Bejan, *Int. J. Heat. Mass. Transfer* **31** (1988) 211.
  8. J.A. Rocha-Martínez, T.D. Navarrete-González, and F. Angulo-Brown, *Rev. Mex. Fís.* **42** (1996) 588.
  9. M.A. Barranco-Jiménez and F. Angulo-Brown, *Rev. Mex. Fís.* **51** (2005) 49.
  10. J.C. Chimal-Eguía, M.A. Barranco-Jiménez, and F. Angulo-Brown, *Open Sys. and Information Dyn.* **13** (2006) 43.
  11. M.A. Barranco-Jiménez, J.C. Chimal-Eguía, and F. Angulo-Brown, *Rev. Mex. Fís.* **52** (2006) 205.
  12. A. De Vos, *Am. J. Phys.* **53** (1985) 570.
  13. J. Chen *et al.*, *Applied Energy.* **81** (2005) 388.
  14. M.A. Barranco-Jiménez and F. Angulo-Brown, *J. Energy Inst.* **80** (2007) 96.
  15. F. Angulo-Brown and R. Paéz-Hernández, *J. Appl. Phys.* **74** (1993) 2216.
  16. M. Huleihil and B. Andresen, *J. Appl. Phys.* **100** (2006) 014911.
  17. L.A. Arias-Hernández, G. Ares de Parga, and F. Angulo-Brown, *J. Appl. Phys.* **101** (2007) 036106-036106-2.
  18. A.Z. Sahin, *Energy Conversion and Management* **41** (2000) 1335.
  19. O.S. Sogut and A. Durmayaz, *J. Energy Institute.* **79** (2006) 246.
  20. C.O' Sullivan, *Am. J. Phys.* **38** (1990) 956. In this article a discussion of the differences between the Newton's law of cooling and the so-called Dulong-Petit heat transfer law is presented.
  21. C. Hu, L. Chen, and J. Chen, *Recent Advances in Finite-Time Thermodynamics* (Nova Science Publishers, Inc, 1999).
  22. M. Fischer and K.H. Hoffmann: *J. Non-Equilib. Thermodyn.* **29** (2004) 9.
  23. A. Durmayaz *et al.*, *Progress in Energy and Combustion Science* **30** (2004) 175.
  24. F. Angulo-Brown, L.A. Arias-Hernández, and M. Santillán-Zerón, *Rev. Mex. Fís.* **48**(S1) (2002) 182.